Report

Cell Reports

Cohesin Removal along the Chromosome Arms during the First Meiotic Division Depends on a NEK1-PP1γ-WAPL Axis in the Mouse

Graphical Abstract

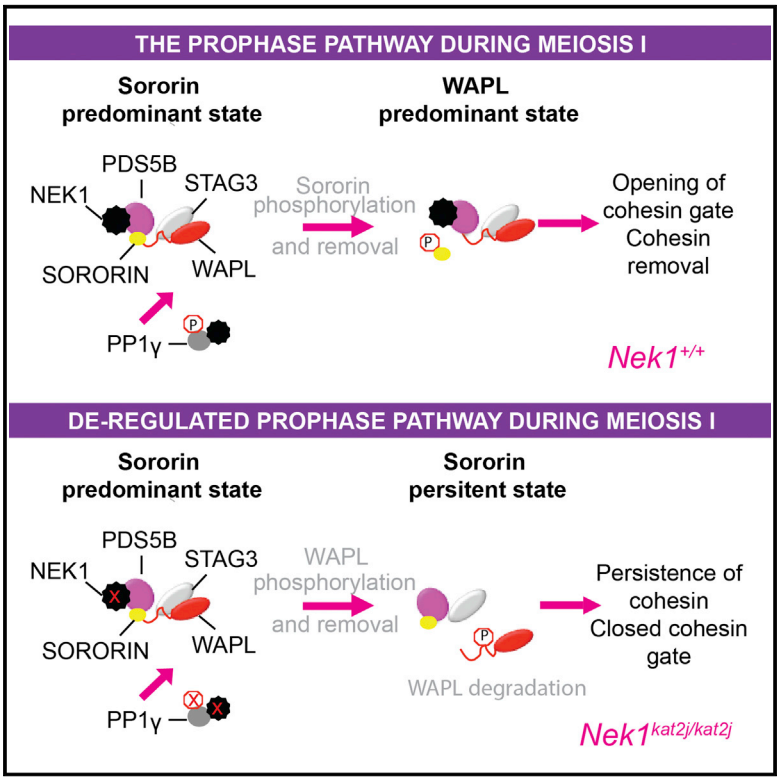

Highlights

- Loss of NEK1 induces retention of cohesin SMC3 and RAD21L
- *Nek1*$^{kat2j/kat2j}$ mice show a premature release of WAPL and retention of sororin
- *Nek1*$^{kat2j/kat2j}$ mice show higher levels of WAPL phosphorylation
- *Nek1*$^{kat2j/kat2j}$ mice show a reduction of PP1γ protein levels and phosphorylation

Authors

Miguel A. Brieño-Enríquez, Stefannie L. Moak, Melissa Toledo, ..., José L. Barbero, Paula E. Cohen, J. Kim Holloway

Correspondence

paula.cohen@cornell.edu (P.E.C.), jkh44@cornell.edu (J.K.H.)

In Brief

Brieño-Enríquez et al. identify a role for NEK1 in the regulation of WAPL during meiotic prophase I, via an interaction between NEK1 and PDS5B. Regulation of WAPL by NEK1-PDS5B is mediated by the phosphatase PP1γ. NEK1 phosphorylates PP1γ, leading to the dephosphorylation of WAPL and promoting loss of cohesion at prophase I.

Brieño-Enríquez et al., 2016, Cell Reports *17*, 977–986
October 18, 2016 © 2016 The Author(s).
http://dx.doi.org/10.1016/j.celrep.2016.09.059

Cell Reports
Report

OPEN ACCESS
CellPress

Cohesin Removal along the Chromosome Arms during the First Meiotic Division Depends on a NEK1-PP1γ-WAPL Axis in the Mouse

Miguel A. Brieño-Enríquez,[1] Stefannie L. Moak,[1] Melissa Toledo,[1] Joshua J. Filter,[2] Stephen Gray,[1] José L. Barbero,[3] Paula E. Cohen,[1,4,*] and J. Kim Holloway[1,*]
[1]Department of Biomedical Sciences and Center for Reproductive Genomics, Cornell University, Ithaca, NY 14853, USA
[2]Department of Molecular Biology and Genetics, Cornell University, Ithaca, NY 14853, USA
[3]Department of Cellular and Molecular Biology, Laboratory of Chromosomal Dynamics in Meiosis, Centro de Investigaciones Biológicas (CSIC), Madrid 28040, Spain
[4]Lead Contact
*Correspondence: paula.cohen@cornell.edu (P.E.C.), jkh44@cornell.edu (J.K.H.)
http://dx.doi.org/10.1016/j.celrep.2016.09.059

SUMMARY

Mammalian NIMA-like kinase-1 (NEK1) is a dual-specificity kinase highly expressed in mouse germ cells during prophase I of meiosis. Loss of NEK1 induces retention of cohesin on chromosomes at meiotic prophase I. Timely deposition and removal of cohesin is essential for accurate chromosome segregation. Two processes regulate cohesin removal: a non-proteolytic mechanism involving WAPL, sororin, and PDS5B and direct cleavage by separase. Here, we demonstrate a role for NEK1 in the regulation of WAPL loading during meiotic prophase I, via an interaction between NEK1 and PDS5B. This regulation of WAPL by NEK1-PDS5B is mediated by protein phosphatase 1 gamma (PP1γ), which both interacts with and is a phosphotarget of NEK1. Taken together, our results reveal that NEK1 phosphorylates PP1γ, leading to the dephosphorylation of WAPL, which, in turn, results in its retention on chromosome cores to promote loss of cohesion at the end of prophase I in mammals.

INTRODUCTION

Meiosis is a specialized cell division characterized by a single round of DNA replication followed by two rounds of chromosome segregation, resulting in the formation of haploid gametes. In order to achieve accurate segregation at both divisions, tension must be established on the meiotic spindles, which is achieved by the formation of crossovers between homologous chromosomes in prophase I of meiosis, and by cohesion between sister chromatids in both meiosis I and meiosis II. Cohesion is established by the cohesin complex and is an essential component of prophase I events, along with the defining feature of prophase I: the synaptonemal complex. Early in prophase I of meiosis, a proteinaceous structure called the axial element (AE) begins to form along replicated sister chromatids, consisting of proteins such as synaptonemal complex proteins-2 and -3 (SYCP2 and SYCP3), along with several cohesin components. Subsequently, the AEs of homologous chromosomes become juxtaposed by proteins of the central element of the synaptonemal complex (SYCP1, TEX12, etc.). The paired AEs, now termed lateral elements (LEs), are now joined by the transverse elements of the central element, collectively forming the tripartite synaptonemal complex (SC) that connects all homologs at pachytene (Llano et al., 2012).

Timely deposition and removal of cohesin is essential for SC dynamics and for accurate chromosome segregation during both mitosis and meiosis. Cohesin complexes differ in mitosis compared to meiosis, consisting of SMC3, SMC1α, STAG1/2, and RAD21 in the former (Haering and Jessberger, 2012; Hirano, 2015; Nasmyth and Haering, 2009) and consisting of REC8, RAD21L, STAG3, SMC1α/β, and SMC3 in the latter (Haering and Jessberger, 2012; McNicoll et al., 2013). Cohesin removal during mitosis is a two-step process, beginning in prophase (the "prophase pathway") and continuing with separase-mediated proteolytic cleavage of centromeric cohesin during the metaphase-anaphase transition. During mitosis, the prophase pathway mediates cohesin removal via a non-enzymatic process that involves the cohesin-associated proteins, WAPL (Wings apart-like homolog), PDS5B (Sister chromatid cohesion protein PDS5 homolog B), and sororin (Tedeschi et al., 2013). WAPL facilitates the unloading of cohesin through an antagonistic mechanism that involves competition with sororin for binding to PDS5B (Nishiyama et al., 2010). In mitotic prophase, sororin is phosphorylated by cyclin-dependent kinase (CDK) 1 (CDK1) and Aurora kinase B (AURKB), which results in its release from PDS5B, thus allowing the interaction of WAPL and PDS5B that leads to cohesin release (Dreier et al., 2011; Nishiyama et al., 2013). Thus, sororin-PDS5B interactions mediate cohesin loading/stabilization, while WAPL-PDS5B interactions mediate cohesin unloading.

WAPL is highly expressed in mouse testis and is localized to meiotic chromosome cores during zygotene and pachytene of

This is an open access article under the CC BY-NC-ND license (http://creativecommons.org/licenses/by-nc-nd/4.0/).

prophase I in the mouse (Kuroda et al., 2005). In mouse oocytes, WAPL colocalizes with SYCP2 during pachytene (Zhang et al., 2008). PDS5B is present in spermatogonia and spermatocytes, and during meiotic prophase, it is associated with the AE independently of the presence of synaptonemal complex proteins (Fukuda and Hoog, 2010). Sororin is also localized within the central element of the SC independently of the presence of cohesin (Gómez et al., 2016). However, to date, the function of these proteins and the importance of the prophase pathway in mammalian meiosis remain undescribed.

The never-in-mitosis-gene-A (NIMA)-related kinases (NEKs) are a family of serine/threonine kinases involved in mitotic and meiotic events (Fry et al., 2012; Meirelles et al., 2014), the founding member of which is *Aspergillus nidulans* NIMA (Oakley and Morris, 1983). In mammals, there are 11 orthologous *Nek* genes, but *Nek1* is a unique, dual-specificity kinase highly expressed in mouse germ cells (Letwin et al., 1992; Upadhya et al., 2000). We previously showed that NEK1 interacts with FKBP6, a component of the mammalian synaptonemal complex, during prophase I (Crackower et al., 2003; Holloway et al., 2011) Furthermore, our studies of *Nek1*$^{kat2j/kat2j}$ mice showed that the loss of NEK1 induces retention of the cohesin component SMC3 during diplotene (Holloway et al., 2011), leading us to propose a role for NEK1 in the sequential removal of cohesin during meiosis. Here, we demonstrate that the release of cohesin during prophase I is dependent on NEK1 regulation of WAPL during prophase I. This regulation of WAPL by NEK1 is mediated by NEK1-PDS5B interaction and by protein phosphatase 1 gamma (PP1γ), which both interacts with NEK1 and is a phosphotarget thereof. In support of this, loss of PP1γ activity mimics the meiosis I phenotype observed in *Nek1*$^{kat2j/kat2j}$ mice, while overexpression of PP1γ results in retention of WAPL into diplotene and premature release of cohesin subunits. Thus, we have established a phosphorylation cascade regulating timely cohesin removal that involves NEK1-mediated phosphorylation of targets during prophase I. Importantly, this study establishes a role for the prophase pathway in chromosome segregation events during meiosis I.

RESULTS

Loss of NEK1 Induces Abnormal Phosphorylation of WAPL and Premature Release from Chromosome Cores

Loss of NEK1 in mouse spermatocytes leads to abnormal retention of SMC3 on chromosome arms at the diplotene and diakinesis (Figure S1) (Holloway et al., 2011). To identify candidate targets of NEK1 that might affect the removal of cohesin during prophase I, we compared the spectrum of phosphorylated proteins in *Nek1*$^{+/+}$ and *Nek1*$^{kat2j/kat2j}$ littermate testes by mass spectrometry (MS) (Figure 1A; Table S1). A total of 445 proteins were found to have abnormal phosphorylation profiles in the mutants compared to WT mice, with 105 proteins showing increased phosphorylation in the mutant protein extracts and 340 showing a reduction in phosphorylation. Of particular relevance to the persistent cohesin retention was the prophase pathway component, WAPL, which showed an abnormal elevation in phosphorylation at the serine residue in position 226 (Figure 1A). In light of the well-documented role of WAPL in cohesin release in mitotic cells, deregulation of WAPL during meiosis would be well placed to be causative for the abnormal persistence of cohesin during prophase I. Moreover, no direct post-translational regulation of WAPL, such as we describe herein, has been reported, either in mitosis or in meiosis. Confoundingly, however, the fact that loss of NEK1 kinase activity leads to increased phosphorylation of WAPL, rather than a predicted decline in phosphorylation, led us to predict that WAPL was not a direct target of NEK1 but might be phosphorylated or dephosphorylated by another protein that is, itself, a target of NEK1. Therefore, we performed an immunoprecipitation (IP) experiment with an antibody against NEK1 in both mutant and WT mouse testis extracts followed by MS (proteins that appear in both IP-MS results were considered as false positive and eliminated) (Table S2). Interestingly, our results demonstrated that PDS5B is a binding partner of NEK1, whereas WAPL is not. The NEK1-PDS5B interaction and lack of interaction between NEK1 and WAPL were both confirmed by IP followed by western blotting (WB) (Figure S2).

The proteomics data described earlier indicate a physical interaction between PDS5B and NEK1, and at least a functional (though indirect) interaction between WAPL and NEK1, leading us to hypothesize that WAPL/PDS5B interactions with NEK1 might explain the retention of SMC3 during prophase I. To examine this further, chromosome spreads were prepared from spermatocytes of both *Nek1*$^{kat2j/kat2j}$ mice and *Nek1*$^{+/+}$ mice and were subjected to immunofluorescence (IF) using antibodies against components of the prophase pathway (PDS5B, WAPL, and sororin). The distribution of PDS5B observed in our studies was similar to that described previously (Fukuda and Hoog, 2010), with no difference being observed in the temporal distribution or frequency of PDS5B loading on chromosome cores in *Nek1*$^{kat2j/kat2j}$ mice compared to *Nek1*$^{+/+}$ mice (Figure 1A). The presence and dynamics of WAPL protein localization were evaluated in both WT and mutant animals. In *Nek1*$^{+/+}$ male spermatocytes, WAPL is observed from leptotene to pachytene of prophase I, colocalizing with SYCP3 along the chromosome cores independently of the synapsis. Finally, at diplotene, WAPL is removed from chromosome cores (Figure 1C). However, in the absence of NEK1, WAPL shows premature release from the chromosome cores in early prophase I, as early as late zygotene in *Nek1*$^{kat2j/kat2j}$ males (Figure 1C).

Release of cohesion via the prophase pathway represents a balance between WAPL and sororin (Nishiyama et al., 2010). Given the premature release of WAPL from PDS5B in the absence of NEK1, we evaluated the localization of sororin by IF. Indeed, analysis of chromosome spreads shows the retention of sororin along cores during pachytene in the *Nek1*$^{kat2j/kat2j}$ mice compared to WT littermates (Figure 1D). Our data are consistent with the requirement for sororin removal in order to facilitate cohesin removal at the end of prophase I, with a stronger and more persistent signal of sororin found in *Nek1*$^{kat2j/kat2j}$ spermatocytes. The changes we observed in the dynamics of WAPL and sororin presence during late prophase I were analyzed by WB of protein extracts from isolated pachytene spermatocytes, with WAPL showing a decrease in protein abundance in *Nek1*$^{kat2j/kat2j}$ mice (Figure S2B). By contrast, sororin shows a subtle increase in protein abundance in extracts from *Nek1*$^{kat2j/kat2j}$ males, while no

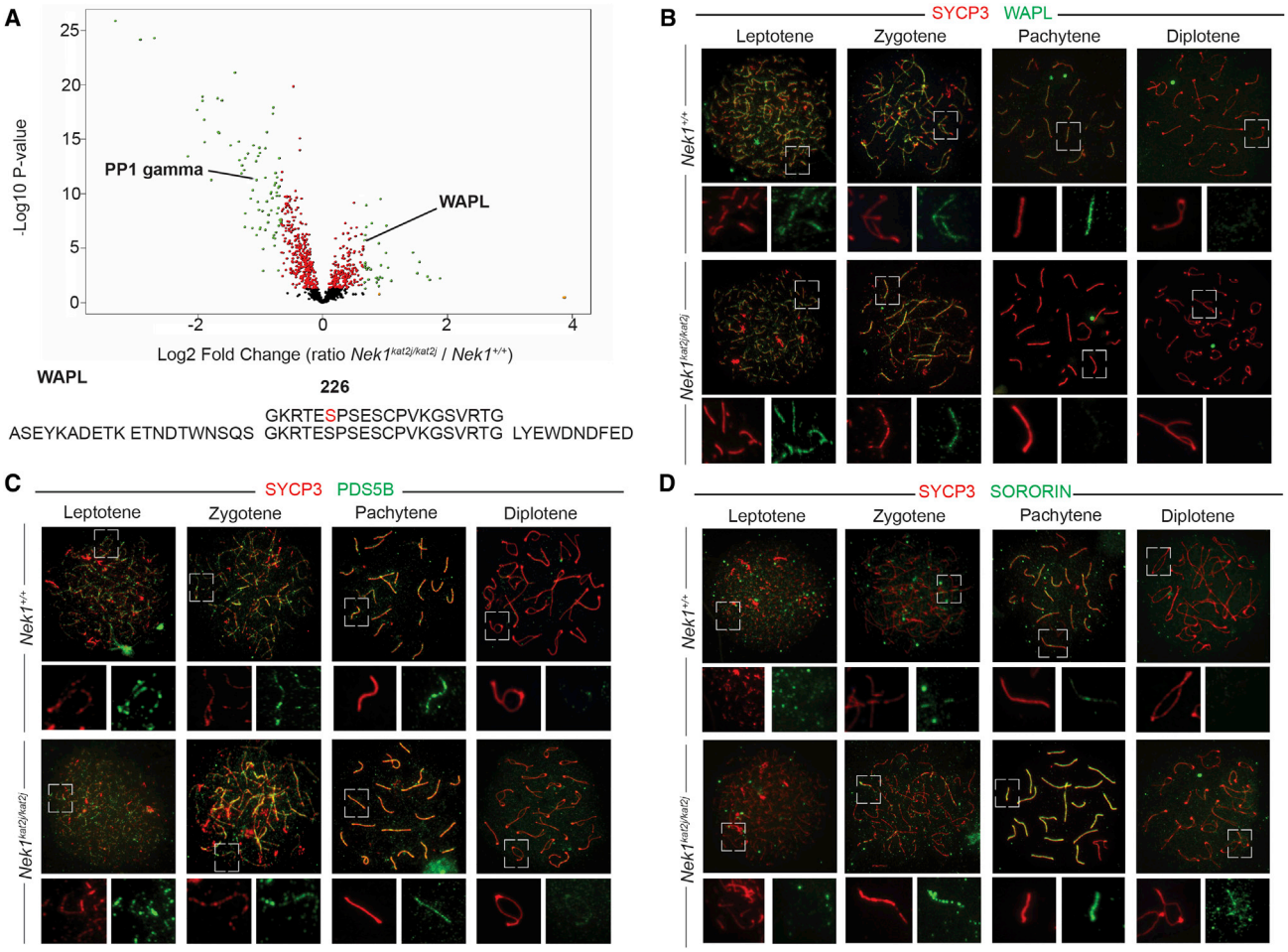

Figure 1. Loss of NEK1 Induces Changes in Phosphorylation Profile, Provoking a Premature Removal of WAPL from Chromosome Cores and Retention of Sororin

(A) Distribution of phosphoproteins analyzed by mass spectrometry. Black dots indicate detected phosphopeptides without changes in $-\log_{10}$ of p value or fold change (FC); red dots indicate $p > 0.05$ without change in $\log_2$ FC; orange dots show $-\log_{10}$ of $p > 0.05$ and $\log_2$ FC > 1. Green dots indicate $-\log_{10}$ of $p > 0.05$ and $\log_2$ FC > 1 ($n = 3$).

(B) IF against WAPL (green) and SYCP3 (red) in spermatocyte spreads from *Nek1*$^{+/+}$ and *Nek1*$^{kat2j/kat2j}$ male mice.

(C) IF against PDS5B (green) and SYCP3 (red) in spermatocyte spreads from *Nek1*$^{+/+}$ and *Nek1*$^{kat2j/kat2j}$ male mice.

(D) IF against sororin (green) and SYCP3 (red) in spermatocyte spreads from *Nek1*$^{+/+}$ and *Nek1*$^{kat2j/kat2j}$ male mice.

See also Figures S1 and S4 and Table S1.

changes were observed in PDS5B protein extracts from *Nek1*$^{kat2j/kat2j}$ relative to that seen in WT extracts (Figure S2B). Localization of all three components of the prophase pathway (WAPL, PDS5B, and sororin) is coincident with the localization of NEK1 described previously (on chromosome cores and increased signal at the sex body) (Yeo et al., 2015).

Identification of PP1γ as a Candidate Phosphatase that Is a Target of NEK1

The aforementioned data demonstrate that loss of NEK1 results in abnormal phosphorylation of WAPL. We hypothesize that this aberrant phosphorylation leads to the premature release of WAPL from chromosome cores during prophase I, allowing for the retention of sororin, although certainly this is, by no means, the only possible explanation for such an observation. However, the abnormal phosphorylation of WAPL is consistent with the idea that, under physiological conditions, NEK1 could be phosphorylating a phosphatase that promotes the dephosphorylation of WAPL to aid its retention on chromosome cores. To test this hypothesis, IP-MS was performed using an antibody against WAPL (Table S3). Results obtained from WAPL IP-MS (Table S3) were cross-referenced with MS results obtained from the aforementioned phosphoproteomics of NEK1 targets (Table S1) and with NEK1 IP-MS data (Table S2). A single candidate emerged that was present in all three sets of results: PP1γ. PP1γ is reduced in the global MS data from *Nek1*$^{kat2j/kat2j}$ males, is found in the IP-MS data for NEK1 interactors, and shows a reduction in phosphorylation at serine 129 in *Nek1*$^{kat2j/kat2j}$ males

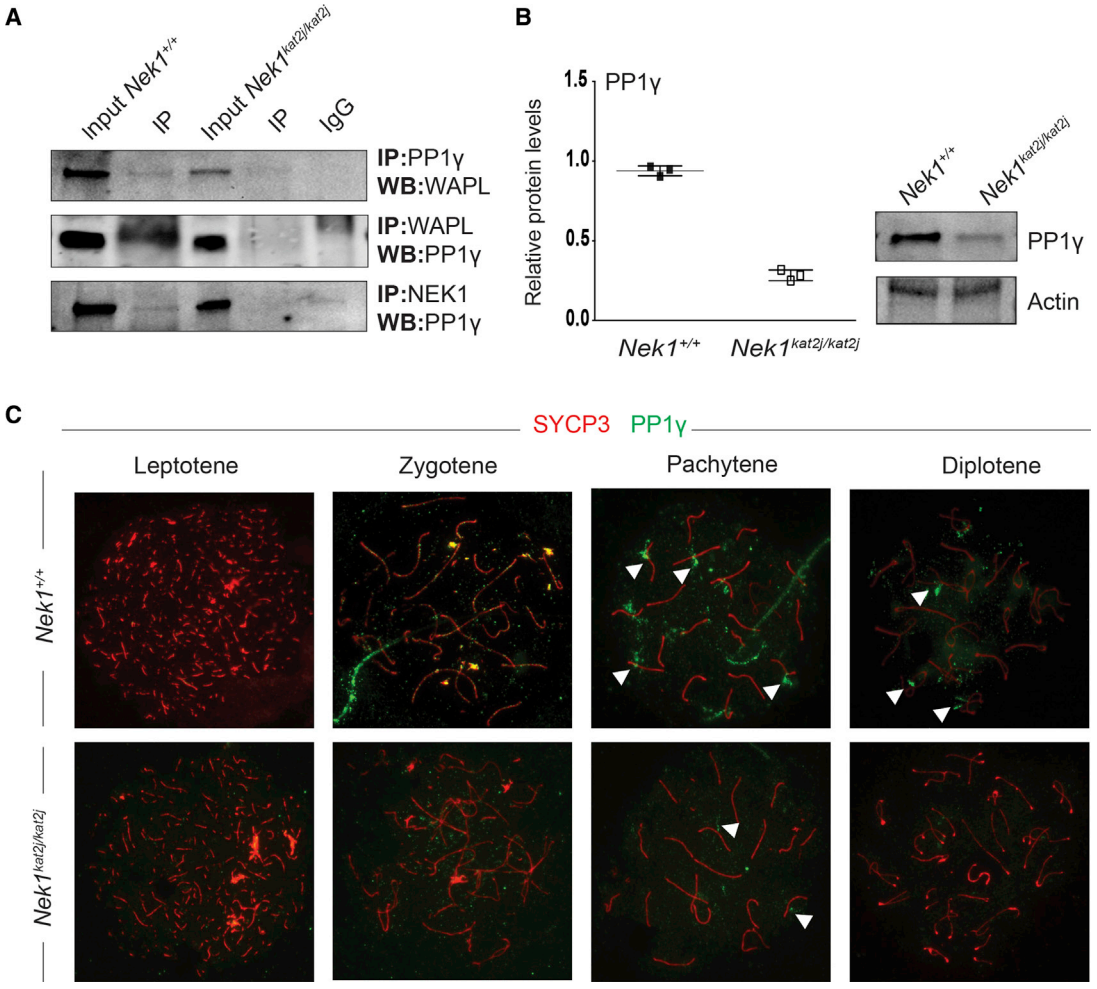

Figure 2. Loss of NEK1 Induces Low Protein Levels and Premature Removal of PP1γ from Chromosome Cores

(A) Immunoprecipitation with WAPL, PP1γ, and NEK1 antibodies, followed by WB.

(B) PP1γ protein levels in isolated pachytene cells from *Nek1*$^{+/+}$ and *Nek1*$^{kat2j/kat2j}$ testes relative to actin (n = 3).

(C) IF against PP1γ (green) and SYCP3 (red) in spermatocytes from *Nek1*$^{+/+}$ and *Nek1*$^{kat2j/kat2j}$ male mice. Arrowheads indicate the flare pattern of PP1γ along chromosome cores from pachytene and diplotene spermatocytes.

See also Figure S2 and Tables S2 and S3.

(Table S1). Thus, PP1γ emerges as a strong candidate to interact with, and become modified (directly or indirectly) by, NEK1 while at the same time potentially phosphorylating WAPL.

Lack of NEK1 Disrupts PP1γ Localization and Levels in Spermatocytes

The interaction between WAPL and PP1γ was confirmed by IP-WB (Figure 2A). Evaluation of total protein level revealed a significant reduction in PP1γ in protein extracts from isolated pachytene cells from *Nek1*$^{kat2j/kat2j}$ males, as detected by WB (Figure 2B). In addition, PP1γ localization on chromosome spreads from WT and NEK1-deficient males was demonstrated by IF using antibodies against total PP1γ and was found to be loaded along the chromosome cores in WT males at late zygotene, after which time, the protein signal diminishes and is restricted to occasional "flares" that cross the chromosome axes in a perpendicular direction. These flares are detectable on chromosome spreads until pachytene (Figure 2C). By contrast, chromosome spreads from *Nek1*$^{kat2j/kat2j}$ males show no detectable PP1γ at zygotene, and few cells displaying limited flare pattern at pachytene (Figure 2C).

Inhibition of PP1γ Induces Phosphorylation of WAPL

The identification of PP1γ as an interacting protein for both WAPL and NEK1, its status as a potential phosphotarget for NEK1, and the reduction of PP1γ protein during pachytene in *Nek1*$^{kat2j/kat2j}$ mutants all implicate PP1γ as a candidate phosphatase that might dephosphorylate WAPL during prophase I under normal conditions. Thus, we hypothesized that the reduction in PP1γ levels and/or activity in NEK1-deficient males would result in the WAPL phosphorylation observed during prophase I in these animals. To test this directly, we used a pharmacological approach by

inhibiting PP1γ activity and assaying for the status of WAPL phosphorylation. Spermatocytes from *Nek1*$^{+/+}$ males were cultured for 6 hr in the presence of the pan-phosphatase inhibitors, okadaic acid (OA) and calyculin A (CLA). OA was used at doses that mainly inhibit protein phosphatase 2 (1, 10, and 100 nM), while CLA was used at doses that inhibit PP1 (2 and 20 nM) (Kita et al., 2002; Swingle et al., 2007). WB revealed that CLA significantly reduced the amount of WAPL protein compared to those spermatocytes cultured with vehicle alone (ethanol) (Figure 3A). By contrast, there were no changes in WAPL protein when spermatocytes were cultured in the presence of OA (Figure 3B). Interestingly, IP with anti-phosphoserine antibody followed by WB with an antibody against WAPL revealed that CLA, but not OA, induced increased all the possible forms of phosphorylated WAPL (phospho-WAPL) in short-term cultures of WT spermatocytes (Figure 3C). Thus, pharmacological inhibition of PP1γ using CLA in WT spermatocytes results in increased phospho-WAPL and subsequent destabilization of WAPL protein, supporting the hypothesis that WAPL is a direct target of PP1γ activity.

PP1γ Mutant Mice Showed a Phenotype that Mimics *Nek1* Mutant Mice

To confirm our in vitro inhibitor results, an in vivo genetics approach was used with previously characterized PP1γ knockout mice (*Ppp1cc*$^{-/-}$) (Varmuza et al., 1999). Chromosome spread analysis of WAPL localization in *Ppp1cc*$^{-/-}$ mice phenocopied the spermatocyte phenotypes observed in *Nek1*$^{kat2j/kat2j}$ mice, with premature release of WAPL from the chromosome cores at late zygotene, leaving a faint residual signal during pachytene in the *Ppp1cc*$^{-/-}$ mice compared to WT controls (Figure 3D). WB with an antibody against WAPL on testis protein from *Ppp1cc*$^{-/-}$ mice confirmed these results, with a reduction in the WAPL protein level in the mutant testis extracts compared to that observed in WT testis extracts (Figure 3E). IP with anti-phosphoserine antibody followed by WB with an antibody against WAPL confirmed an increase in phospho-WAPL in the spermatocytes of *Ppp1cc*$^{-/-}$ mice (Figure 3F). To test indirectly the activity of PP1γ on WAPL and SMC3, we performed IF in the previously described *Ppp1cc* overexpressing PPP1CC2 mouse (*Ppp1cc*$^{+/+Tg(Ppp1cc2/Ppp1cc2)}$) (Sinha et al., 2013). Our results show that PP1γ overexpression leads to the retention of WAPL into diplotene and release of SMC3 (Figure S3). Thus, these data demonstrate that the absence of NEK1, or of PP1γ phosphatase activity, results in abnormal phosphorylation of WAPL, leading to premature release of WAPL from chromosome cores in late prophase I, disrupting the prophase pathway in mouse meiosis.

DISCUSSION

During mitosis, WAPL is a constituent of the prophase pathway (Gandhi et al., 2006; Huis in 't Veld et al., 2014; Kueng et al., 2006; Tedeschi et al., 2013), forming a complex with PDS5B to facilitate the unloading of cohesin during prophase (Carretero et al., 2013; Shintomi and Hirano, 2009). During S phase, WAPL-PDS5B function is antagonized by sororin, which displaces WAPL from PDS5B, thereby promoting cohesin loading and/or stabilization (Shintomi and Hirano, 2009; Zhang et al., 2008). Recent studies in *Caenorhabditis elegans*, *Saccharomyces cerevisiae*, and *Arabidopsis thaliana* demonstrated a role for WAPL in cohesin regulation during meiosis (Challa et al., 2016; Crawley et al., 2016; De et al., 2014). In *C. elegans* oogenesis, WAPL-1 antagonizes the binding of cohesin containing the COH-3/4 kleisins, but not REC-8, and promotes a WAPL-1-independent mechanism that removes cohesin before metaphase I (Crawley et al., 2016). In *S. cerevisiae*, the ortholog of WAPL (Rad61/Wpl1) negatively regulates chromosome axis compaction and is required for the efficient resolution of telomere clustering during meiosis I (Challa et al., 2016). Mutation of WAPL in *A. thaliana* blocks the removal of cohesin from chromosomes during meiosis, resulting in chromosome bridges, broken chromosomes, and uneven chromosome segregation (De et al., 2014). However, studies in the mouse have been limited only to a brief description of WAPL localization on chromosome core (Kuroda et al., 2005; Zhang et al., 2008). Here, we demonstrate that loss of NEK1 results in abnormal phosphorylation of WAPL, which leads to premature loss of WAPL from the chromosome cores and reduction of protein levels in prophase I (Figure 1C). The premature release of WAPL in the absence of NEK1 allows for the persistence of sororin (Figure 1D) and subsequent retention of SMC3 during diplotene and diakinesis (Figure S1). Our data also indicate that NEK1 mutant spermatocytes retain RAD21L on meiotic chromosome cores at the end of prophase I (Figure S4), indicating that SMC3 is not the only cohesin subunit to be disrupted. Post-translational modifications of WAPL have been described in the phosphoproteomics screening of polo-like kinase targets (Grosstessner-Hain et al., 2011) and in PP1γ mutant mice (MacLeod et al., 2014). However, the role of such regulation of WAPL has not been described in mammalian meiosis, nor have changes in the phosphoproteomic profile of WAPL been associated with prophase I defects in the mouse. Alignment of WAPL orthologs across species (Figure S5) shows conservation of serine 226 in mouse and human but within a larger domain of other conserved serines (for example, serine 228 and serine 236). In all, at least five serine residues in this region are conserved across mammals and in *D. melanogaster*, providing the potential for this region to be highly regulated by phosphorylation events.

Interaction between PDS5B and WAPL is mediated by HEAT repeats (Losada et al., 2005; Nishiyama et al., 2010; Shintomi and Hirano, 2009) and by a YSR motif (Ouyang et al., 2016) on PDS5B. These domains interact with three FGF motifs of WAPL, none of which include the serine 226 identified herein. Thus, NEK1 activity through PP1γ is not directed to the FGF repeats in WAPL. Instead, we propose that phosphorylation of serine 226, or of any of the other highly conserved serines in the vicinity of serine 226, could induce a conformational change in the WAPL protein that destabilizes its interaction with PDS5B, allowing PDS5B-sororin interactions to predominate and resulting in cohesin retention. Alternatively, WAPL phosphorylation could act as a signal for WAPL degradation, resulting in its premature removal from chromosome cores. Finally, the phosphorylation of WAPL at serine 226 may act to suppress key phosphorylation events on other residues. Taken together, our studies implicate a direct regulatory action on WAPL itself, leading to activation of the prophase pathway rather than an indirect

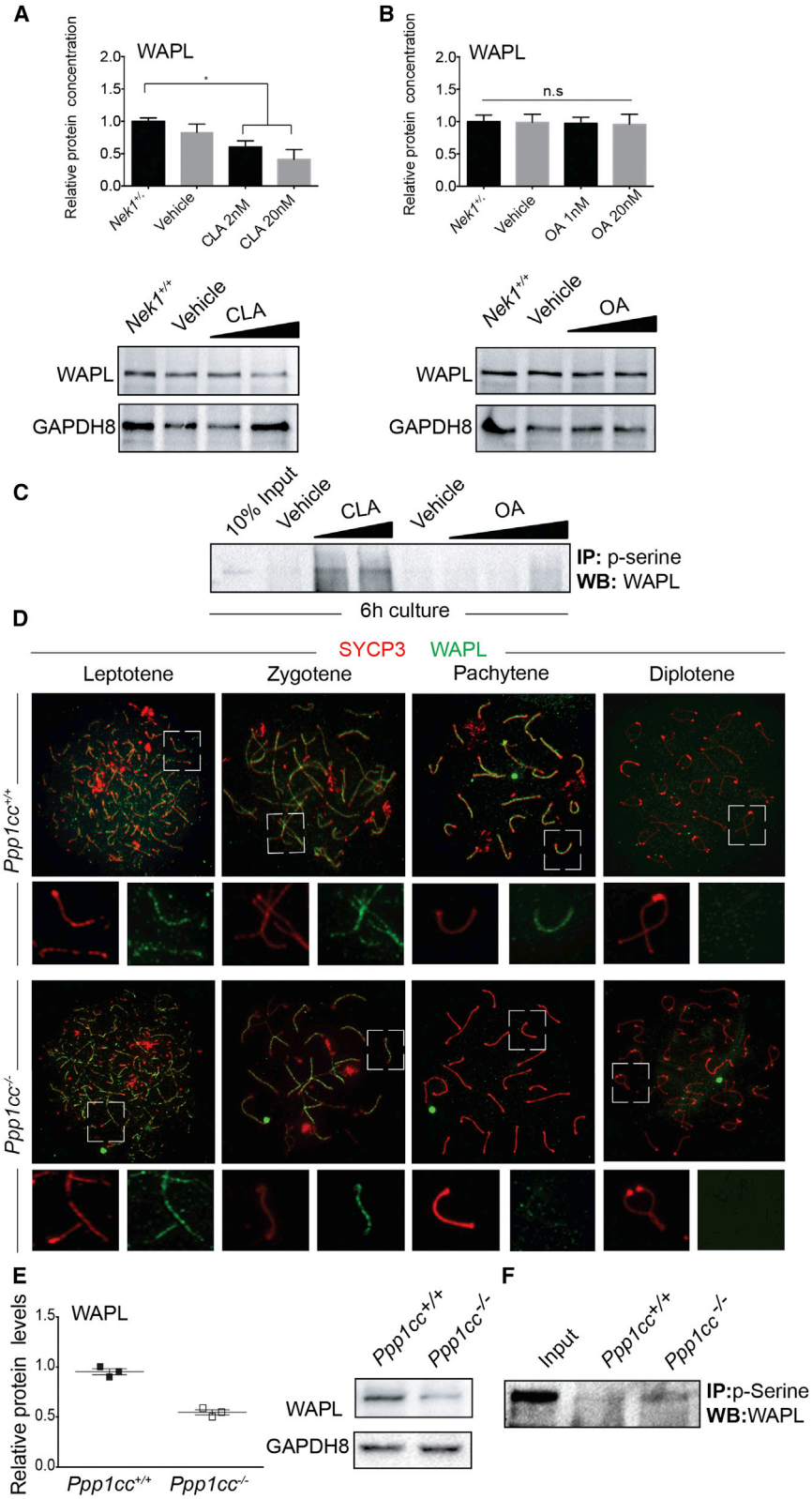

Figure 3. Increased WAPL Phosphorylation Is Caused by the Lack of Phosphorylation of PP1γ by NEK1

(A) Quantitation of WAPL protein levels in extracts from *Nek1*$^{+/+}$ testes relative to GAPDH control in cultured spermatocytes treated with calyculin A (CLA; 2–20 nM) (n = 5).

(B) Quantitation of WAPL protein levels in extracts from *Nek1*$^{+/+}$ testes relative to GAPDH control in cultured spermatocytes treated with okadaic acid (n = 5).

(C) In vitro phosphorylation of WAPL in cultured spermatocytes vehicle (ethanol), calyculin A (CLA) (2 and 20 nM), and okadaic acid (OA) (1, 10, and 100 nM), analyzed by immunoprecipitation pull-downs with antibody against phospho-serine followed by WB. Input lane represents spermatocyte protein extracts without immunoprecipitation.

(D) IF against WAPL (green) and SYCP3 (red) in spermatocytes from *Ppp1cc*$^{+/+}$ and *Ppp1cc*$^{-/-}$ male mice.

(E) Quantitation of WAPL protein levels relative to GAPDH control in extracts from *Ppp1cc*$^{+/+}$ and *Ppp1cc*$^{-/-}$ testes using antibody against WAPL (n = 3).

(F) In vivo phosphorylation of WAPL in *Ppp1cc*$^{+/+}$ and *Ppp1cc*$^{-/-}$ whole testis lysate using immunoprecipitation pull-downs with antibody against phospho-serine followed by western blotting.

*Statistically significant differences (one-way ANOVA followed by Dunnett's multiple comparisons test, $p < 0.05$).

See also Figure S3.

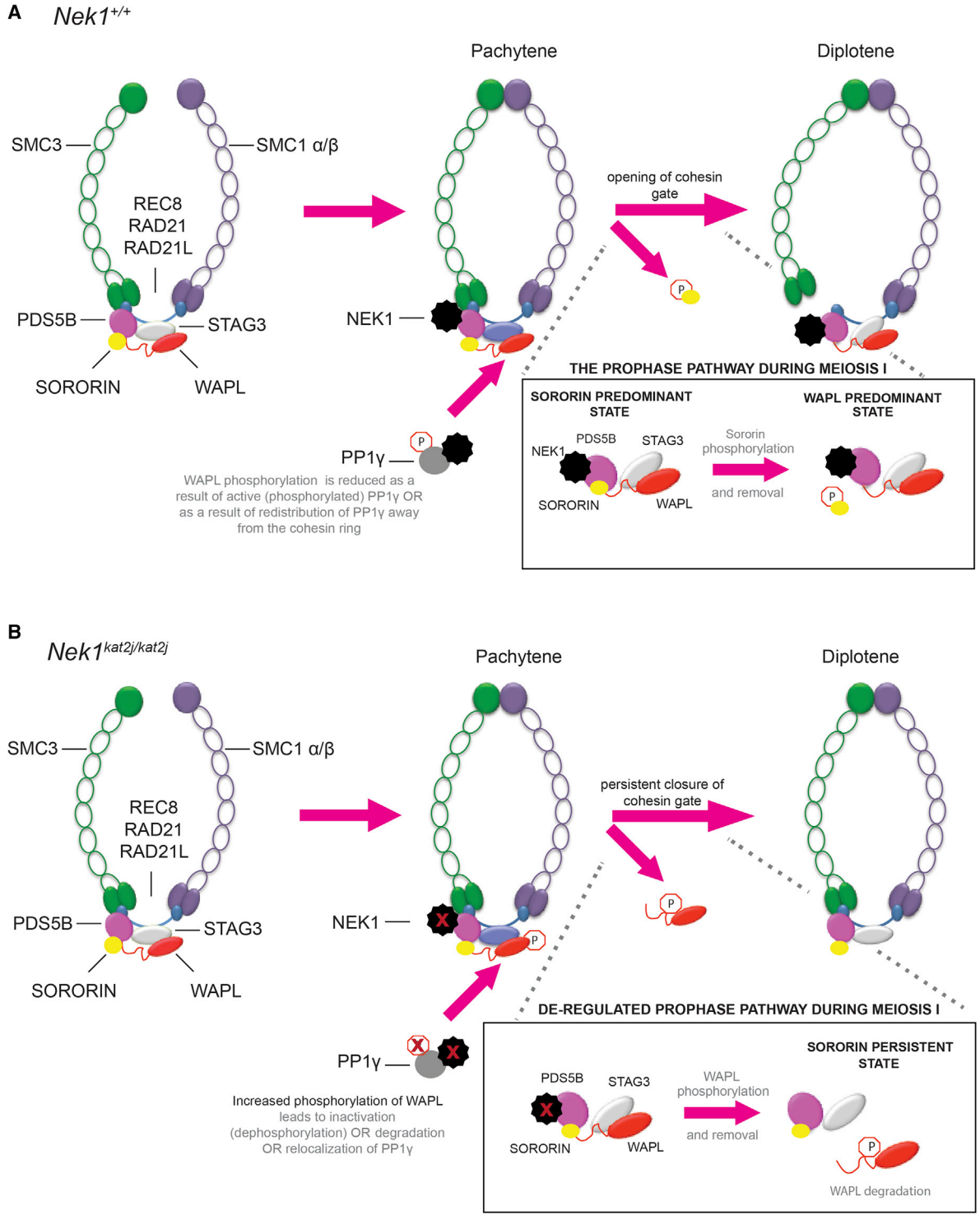

Figure 4. Model the Role of NEK1 during Meiotic Prophase I

(A) Top panel represents the role of NEK1 during meiotic prophase I in WT mice. During prophase I, NEK1 binds to PDS5B at the cohesin ring. Additionally, NEK1 binds to PP1γ and phosphorylates it; phosphorylation of PP1γ subsequently inhibits WAPL phosphorylation and permits its activity during the prophase-metaphase transition without changes in sororin.

(B) The bottom panel represents the effects of loss of NEK1, which results in retention of SMC3. The absence of NEK1 prevents PP1γ phosphorylation which, in turn, permits a hyper-phosphorylation of WAPL. Hyper-phosphorylation of WAPL affects its stability and/or binding to PDS5B, inducing a premature removal of WAPL from the cohesin ring and persistence of sororin. Light gray text denotes events that require further confirmatory studies.

action through regulation of sororin, as has previously been described in other cell systems (Nishiyama et al., 2010; Rankin et al., 2005; Zhang and Pati, 2012).

The data presented herein demonstrate a role for NEK1 during meiotic prophase I, regulating—directly or indirectly—the proteins involved in the prophase pathway, specifically in regulation of the PDS5B-WAPL complex. Importantly, NEK1 function on the PDS5B-WAPL complex appears predicated on its interaction with PDS5B, yet PDS5B itself is not a target of either of the two-kinase activities of NEK1. Instead, our data indicate that this function could be mediated through NEK1 interaction with PP1γ and through the altered phosphorylation status of PP1γ. During mitosis, PP1γ phosphorylation is orchestrated preferentially by CDKs (Dohadwala et al., 1994; Eto, 2009; Kim et al., 2003; Li et al., 2007). However, our phosphoproteomics analysis did not reveal any changes in the phosphorylation status of CDKs in the absence of NEK1. Moreover, the NEK1 IP data failed to identify a candidate CDK that could be a potential substrate for NEK1, and/or kinase for PP1γ. It is highly unlikely, therefore, that PP1γ is phosphorylated by a canonical CDK during meiotic prophase. Instead, we propose that PP1γ is a substrate of NEK1, or that another kinase is acting as an intermediary between these two proteins. Our analysis of the phosphoproteomics and NEK1-IP data failed to reveal such a candidate kinase, but it is possible, as with many kinase-substrate interactions, that NEK1-substrate interactions may be too rapid/transient to permit their identification by IP-MS. Another important factor is the regulation of PP1γ by its regulatory subunits and natural inhibitors. Our MS results showed that there are changes in the protein levels of some of these regulatory subunits and that these may, in turn, regulate the activity or abundance of PP1γ. Thus, analysis of NEK1/PP1γ/WAPL interactions during meiosis are made more complex by involvement of a complex PP1 regulatory network, the particularly large size of the protein constituents of this network, and the potential for multiple serines on WAPL to be the targets of PP1γ activity.

In summary, we propose a model whereby NEK1 docks with PDS5B to bring it into close proximity with the cohesin ring, whereupon it phosphorylates a number of direct targets, altering the phosphorylation status of PP1γ and, hence, its localization and/or activity. PP1γ, in turn, dephosphorylates WAPL, securing its interaction with PDS5B and displacing sororin, resulting in accurate and timely opening of the cohesin ring to facilitate loss of cohesion along the chromosome arms at the end of meiosis I (Figure 4).

EXPERIMENTAL PROCEDURES

All mouse studies were conducted with the prior approval of the Cornell Institutional Animal Care and Use Committee (protocol 2010-0054). The *Nek1*$^{kat2j/kat2j}$ mouse line was obtained originally from The Jackson Laboratory and maintained on a C57Bl/6J line for >10 years at Cornell University. At least three sets of 8-week-old homozygous mutant animals (*Nek1*$^{kat2J/kat2J}$) were compared with WT (*Nek1*$^{+/+}$) littermates. *Ppp1cc*$^{-/-}$ *and* *Pppc1*$^{+/+Tg(Ppp1cc2/Ppp1cc2)}$ mice were generously donated by Dr. Vijayaraghavan (Department of Biomedical Sciences, Kent State University).

Chromosome Spread Preparations and IF Staining

Prophase I spermatocyte chromosome spreads were performed as previously described (Sun et al., 2015). Primary antibodies included: rabbit anti-Sororin (anti-Sororin serum C-106 was generated using a full-length recombinant mouse protein cloned in pET-12a vector and expressed in *E. coli* [Carretero et al., 2013]), anti-mouse SYCP3 (ab97672), rabbit anti-PDS5B (ab84918) (both from Abcam), rabbit anti-WAPL (16370-1-AP, from Proteintech), rabbit anti-PP1γ (PA5-21671, from Thermo Fisher), rabbit anti-SMC3 (from J.L.B.), and rabbit anti-RAD21L (from Alberto Pendás). Alexa Fluor secondary antibodies were used (Molecular Probes). Image acquisition was performed using a Zeiss Imager Z1 microscope and captured using a Zeiss charge-coupled device (CCD). Images were processed using AxioVision (version 4.8, Zeiss).

Isolation of Pachytene Cells

Nek1$^{+/+}$ and *Nek1*$^{kat2j/kat2j}$ enrichment of specific spermatogenic cell types was performed using the STA-PUT method based on separation by cell diameter/density at unit gravity (Bellvé, 1993; Romrell et al., 1976). Purity of resulting fractions was determined by microscopy based on cell diameter and morphology.

Culture of Spermatocytes

Culture was performed following the protocol described elsewhere (Wiltshire et al., 1995), with some modifications. Briefly, we dissociated testes in 4 mL of spermatocyte culture medium (SCM) (DMEM without red phenol [21063-029], fetal calf serum [10082139], penicillin-streptomycin 100× [15140-122], all from GIBCO; lactic acid [L13750, $NaHCO_3$ 9s8761] and sodium pyruvate 100× [11360-070], both from Sigma). Cells were placed in treated culture dishes (#430167, Corning), washed five times with SCM, and centrifuged 1,000 × *g* for 1 min to pellet cells. The pellet was resuspended in 600 μL SCM. 100 μL cell suspension was placed into each 35-mm plate with and without okadaic acid (135 μM, 50 μg/μL) (O9381, Sigma) or with and without calyculin A (2–200 nM) (sc-24000, Santa Cruz Biotechnology). Cells were cultured for 6 hr at 32°C before analysis.

Western Blot and IP

Proteins were extracted by sonication in RIPA buffer, denaturalized, and then separated using 4%–15% Mini-PROTEAN TGX Precast Protein Gels (#4561086, from Bio-Rad) and transferred onto nitrocellulose membrane. Primary antibody incubation was performed for 12 hr at 4°C at 1:1,000 dilution. Secondary HRP (horseradish peroxidase)-conjugated antibodies were obtained from Pierce and Life Technologies. Signal detection was carried out using the SuperSignal substrate (Thermo Scientific). Images were captured with Bio-Rad Image Lab 5.1 and analyzed by ImageJ (http://rsbweb.nih.gov/ij). IP was performed using 1 mg of whole testis protein. Incubation with the specific antibody was performed at 4°C overnight. The protein lysate was then centrifuged, and the supernatant was removed. The remaining beads were washed in fresh cold RIPA buffer three times, and the final bead slurry was resuspended in 40 μL 2 × SDS protein loading dye and run in 4%–15% Mini-PROTEAN TGX Precast Protein Gels.

Mass Spectrometry

MS was performed in the Cornell University Proteomics and Mass Spectrometry Facility. Experiments were performed using three different sets of *Nek1*$^{+/+}$ and *Nek1*$^{kat2j/kat2j}$ mice. To obtain the specific postranslational modification of the peptides, we performed TiO2 enrichment followed by the proteomics analysis. After nano-liquid chromatography-tandem MS (nano-LC-MS/MS), raw data files were acquired using Orbitrap Elite (Thermo Scientific). We performed a database search against the SwissProt mouse database from the UniProt website (http://www.uniprot.org) using Mascot software version 2.3.02 (Matrix Science) and MouseRefSeq (http://www.ncbi.nlm.nih.gov/refseq). The default Mascot search settings were as follows:

1. One missed cleavage site by trypsin allowed with fixed MMTS modification of cysteine; fixed 4-plex iTRAQ modifications on Lys and N-terminal amines; and variable modifications of methionine oxidation, deamidation of Asn and Gln residues, and 4-plex iTRAQ on Tyr for iTRAQ 4-plex analysis.
2. One or two missed cleavage sites by trypsin allowed with fixed carboxamidomethyl modification of cysteine; fixed 6-plex TMT modifications

on Lys and N-terminal amines; and variable modifications of methionine oxidation, deamidation of Asn and Gln residues, and 6-plex TMT on Tyr for TMT 6-plex analysis.
3. Peptide mass tolerance was set at 0.01 Da, and fragment mass tolerance was set at 0.1 Da; decoy search: yes; ion score cutoff: 0.1.
4. The quantitative protein ratios were weighted and normalized by the median ratio with outlier removal set automatically in Mascot for each set of experiments.

We performed NEK1-IP on three different protein sets (from three distinct mice) following the parameters described earlier. Quantification analysis of NEK1-IP was performed following the label-free quantitation analysis using MaxQuant software (Max Planck Institute of Biochemistry; http://www.biochem.mpg.de/5111795/maxquant).

Statistics

Statistical analyses were performed using GraphPad Prism version 6.00 for Macintosh (GraphPad Software; http://www.graphpad.com).

SUPPLEMENTAL INFORMATION

Supplemental Information includes five figures and three tables and can be found with this article online at http://dx.doi.org/10.1016/j.celrep.2016.09.059.

AUTHOR CONTRIBUTIONS

M.A.B.-E., P.E.C., and J.K.H. designed experiments. M.A.B.-E., S.L.M., M.T., J.J.F., and S.G. carried out the experiments. M.A.B.-E., S.L.M., P.E.C., and J.K.H. analyzed and interpreted data. J.L.B. provided critical antibodies. M.A.B.-E. and P.E.C. wrote the manuscript.

ACKNOWLEDGMENTS

We thank Dr. Lee Zhou for the anti-NEK1 antibody, Dr. Ana Losada for the anti-Sororin antibody, Dr. Alberto Pendás for the anti-RAD21L antibody, Dr. Srinivasan Vijayaraghavan for *Ppp1cc*$^{-/-}$ and *Ppp1cc*$^{+/+Tg(Ppp1cc2/Ppp1cc2)}$ mice, Dr. Michael Goldberg for advice and reagents pertaining to PP1γ analysis, and Dr. Sheng Zhang from the Cornell Proteomics and Mass Spectrometry Facility for his advice in the development of MS experiments. We thank Mr. Peter Borst for his help in the care and maintenance of experimental animals. This project is funded by grants from the NICHD to J.K.H. (5R00HD065870) and from NIGMS and March of Dimes to P.E.C. (1R01GM097263 and MOD2006-844). J.L.B. is funded by a grant from MINECO (BFU2014-59307), Spain.

Received: April 29, 2016
Revised: July 25, 2016
Accepted: September 16, 2016
Published: October 18, 2016

REFERENCES

Bellvé, A.R. (1993). Purification, culture, and fractionation of spermatogenic cells. Methods Enzymol. *225*, 84–113.

Carretero, M., Ruiz-Torres, M., Rodríguez-Corsino, M., Barthelemy, I., and Losada, A. (2013). Pds5B is required for cohesion establishment and Aurora B accumulation at centromeres. EMBO J. *32*, 2938–2949.

Challa, K., Lee, M.S., Shinohara, M., Kim, K.P., and Shinohara, A. (2016). Rad61/Wpl1 (Wapl), a cohesin regulator, controls chromosome compaction during meiosis. Nucleic Acids Res. *44*, 3190–3203.

Crackower, M.A., Kolas, N.K., Noguchi, J., Sarao, R., Kikuchi, K., Kaneko, H., Kobayashi, E., Kawai, Y., Kozieradzki, I., Landers, R., et al. (2003). Essential role of Fkbp6 in male fertility and homologous chromosome pairing in meiosis. Science *300*, 1291–1295.

Crawley, O., Barroso, C., Testori, S., Ferrandiz, N., Silva, N., Castellano-Pozo, M., Jaso-Tamame, A.L., and Martinez-Perez, E. (2016). Cohesin-interacting protein WAPL-1 regulates meiotic chromosome structure and cohesion by antagonizing specific cohesin complexes. eLife *5*, e10851.

De, K., Sterle, L., Krueger, L., Yang, X., and Makaroff, C.A. (2014). Arabidopsis thaliana WAPL is essential for the prophase removal of cohesin during meiosis. PLoS Genet. *10*, e1004497.

Dohadwala, M., da Cruz e Silva, E.F., Hall, F.L., Williams, R.T., Carbonaro-Hall, D.A., Nairn, A.C., Greengard, P., and Berndt, N. (1994). Phosphorylation and inactivation of protein phosphatase 1 by cyclin-dependent kinases. Proc. Natl. Acad. Sci. USA *91*, 6408–6412.

Dreier, M.R., Bekier, M.E., 2nd, and Taylor, W.R. (2011). Regulation of sororin by Cdk1-mediated phosphorylation. J. Cell Sci. *124*, 2976–2987.

Eto, M. (2009). Regulation of cellular protein phosphatase-1 (PP1) by phosphorylation of the CPI-17 family, C-kinase-activated PP1 inhibitors. J. Biol. Chem. *284*, 35273–35277.

Fry, A.M., O'Regan, L., Sabir, S.R., and Bayliss, R. (2012). Cell cycle regulation by the NEK family of protein kinases. J. Cell Sci. *125*, 4423–4433.

Fukuda, T., and Hoog, C. (2010). The mouse cohesin-associated protein PDS5B is expressed in testicular cells and is associated with the meiotic chromosome axes. Genes (Basel) *1*, 484–494.

Gandhi, R., Gillespie, P.J., and Hirano, T. (2006). Human Wapl is a cohesin-binding protein that promotes sister-chromatid resolution in mitotic prophase. Curr. Biol. *16*, 2406–2417.

Gómez, R., Felipe-Medina, N., Ruiz-Torres, M., Berenguer, I., Viera, A., Pérez, S., Barbero, J.L., Llano, E., Fukuda, T., Alsheimer, M., et al. (2016). Sororin loads to the synaptonemal complex central region independently of meiotic cohesin complexes. EMBO Rep. *17*, 695–707.

Grosstessner-Hain, K., Hegemann, B., Novatchkova, M., Rameseder, J., Joughin, B.A., Hudecz, O., Roitinger, E., Pichler, P., Kraut, N., Yaffe, M.B., et al. (2011). Quantitative phospho-proteomics to investigate the polo-like kinase 1-dependent phospho-proteome. Mol. Cell. Proteomics *10*, M111008540.

Haering, C.H., and Jessberger, R. (2012). Cohesin in determining chromosome architecture. Exp. Cell Res. *318*, 1386–1393.

Hirano, T. (2015). Chromosome dynamics during mitosis. Cold Spring Harb. Perspect. Biol. *7*, pii: a015792.

Holloway, K., Roberson, E.C., Corbett, K.L., Kolas, N.K., Nieves, E., and Cohen, P.E. (2011). NEK1 facilitates cohesin removal during mammalian spermatogenesis. Genes (Basel) *2*, 260–279.

Huis in 't Veld, P.J., Herzog, F., Ladurner, R., Davidson, I.F., Piric, S., Kreidl, E., Bhaskara, V., Aebersold, R., and Peters, J.M. (2014). Characterization of a DNA exit gate in the human cohesin ring. Science *346*, 968–972.

Kim, Y.M., Watanabe, T., Allen, P.B., Kim, Y.M., Lee, S.J., Greengard, P., Nairn, A.C., and Kwon, Y.G. (2003). PNUTS, a protein phosphatase 1 (PP1) nuclear targeting subunit. Characterization of its PP1- and RNA-binding domains and regulation by phosphorylation. J. Biol. Chem. *278*, 13819–13828.

Kita, A., Matsunaga, S., Takai, A., Kataiwa, H., Wakimoto, T., Fusetani, N., Isobe, M., and Miki, K. (2002). Crystal structure of the complex between calyculin A and the catalytic subunit of protein phosphatase 1. Structure *10*, 715–724.

Kueng, S., Hegemann, B., Peters, B.H., Lipp, J.J., Schleiffer, A., Mechtler, K., and Peters, J.M. (2006). Wapl controls the dynamic association of cohesin with chromatin. Cell *127*, 955–967.

Kuroda, M., Oikawa, K., Ohbayashi, T., Yoshida, K., Yamada, K., Mimura, J., Matsuda, Y., Fujii-Kuriyama, Y., and Mukai, K. (2005). A dioxin sensitive gene, mammalian WAPL, is implicated in spermatogenesis. FEBS Lett. *579*, 167–172.

Letwin, K., Mizzen, L., Motro, B., Ben-David, Y., Bernstein, A., and Pawson, T. (1992). A mammalian dual specificity protein kinase, Nek1, is related to the NIMA cell cycle regulator and highly expressed in meiotic germ cells. EMBO J. *11*, 3521–3531.

Li, T., Chalifour, L.E., and Paudel, H.K. (2007). Phosphorylation of protein phosphatase 1 by cyclin-dependent protein kinase 5 during nerve growth factor-induced PC12 cell differentiation. J. Biol. Chem. *282*, 6619–6628.

Llano, E., Herrán, Y., García-Tuñón, I., Gutiérrez-Caballero, C., de Álava, E., Barbero, J.L., Schimenti, J., de Rooij, D.G., Sánchez-Martín, M., and Pendás, A.M. (2012). Meiotic cohesin complexes are essential for the formation of the axial element in mice. J. Cell Biol. *197*, 877–885.

Losada, A., Yokochi, T., and Hirano, T. (2005). Functional contribution of Pds5 to cohesin-mediated cohesion in human cells and Xenopus egg extracts. J. Cell Sci. *118*, 2133–2141.

MacLeod, G., Taylor, P., Mastropaolo, L., and Varmuzaa, S. (2014). Comparative phosphoproteomic analysis of the mouse testis reveals changes in phosphopeptide abundance in response to Ppp1cc deletion. EuPA Open Proteom. *2*, 1–16.

McNicoll, F., Stevense, M., and Jessberger, R. (2013). Cohesin in gametogenesis. Curr. Top. Dev. Biol. *102*, 1–34.

Meirelles, G.V., Perez, A.M., de Souza, E.E., Basei, F.L., Papa, P.F., Melo Hanchuk, T.D., Cardoso, V.B., and Kobarg, J. (2014). "Stop Ne(c)king around": How interactomics contributes to functionally characterize Nek family kinases. World J. Biol. Chem. *5*, 141–160.

Nasmyth, K., and Haering, C.H. (2009). Cohesin: its roles and mechanisms. Annu. Rev. Genet. *43*, 525–558.

Nishiyama, T., Ladurner, R., Schmitz, J., Kreidl, E., Schleiffer, A., Bhaskara, V., Bando, M., Shirahige, K., Hyman, A.A., Mechtler, K., and Peters, J.M. (2010). Sororin mediates sister chromatid cohesion by antagonizing Wapl. Cell *143*, 737–749.

Nishiyama, T., Sykora, M.M., Huis in 't Veld, P.J., Mechtler, K., and Peters, J.M. (2013). Aurora B and Cdk1 mediate Wapl activation and release of acetylated cohesin from chromosomes by phosphorylating Sororin. Proc. Natl. Acad. Sci. USA *110*, 13404–13409.

Oakley, B.R., and Morris, N.R. (1983). A mutation in Aspergillus nidulans that blocks the transition from interphase to prophase. J. Cell Biol. *96*, 1155–1158.

Ouyang, Z., Zheng, G., Tomchick, D.R., Luo, X., and Yu, H. (2016). Structural basis and IP requirement for Pds5-dependent cohesin dynamics. Mol. Cell *62*, 248–259.

Rankin, S., Ayad, N.G., and Kirschner, M.W. (2005). Sororin, a substrate of the anaphase-promoting complex, is required for sister chromatid cohesion in vertebrates. Mol. Cell *18*, 185–200.

Romrell, L.J., Bellvé, A.R., and Fawcett, D.W. (1976). Separation of mouse spermatogenic cells by sedimentation velocity. A morphological characterization. Dev. Biol. *49*, 119–131.

Shintomi, K., and Hirano, T. (2009). Releasing cohesin from chromosome arms in early mitosis: opposing actions of Wapl-Pds5 and Sgo1. Genes Dev. *23*, 2224–2236.

Sinha, N., Puri, P., Nairn, A.C., and Vijayaraghavan, S. (2013). Selective ablation of Ppp1cc gene in testicular germ cells causes oligo-teratozoospermia and infertility in mice. Biol. Reprod. *89*, 128.

Sun, X., Brieno-Enriquez, M.A., Cornelius, A., Modzelewski, A.J., Maley, T.T., Campbell-Peterson, K.M., Holloway, J.K., and Cohen, P.E. (2015). FancJ (Brip1) loss-of-function allele results in spermatogonial cell depletion during embryogenesis and altered processing of crossover sites during meiotic prophase I in mice. Chromosoma *125*, 237–252.

Swingle, M., Ni, L., and Honkanen, R.E. (2007). Small-molecule inhibitors of ser/thr protein phosphatases: specificity, use and common forms of abuse. Methods Mol. Biol. *365*, 23–38.

Tedeschi, A., Wutz, G., Huet, S., Jaritz, M., Wuensche, A., Schirghuber, E., Davidson, I.F., Tang, W., Cisneros, D.A., Bhaskara, V., et al. (2013). Wapl is an essential regulator of chromatin structure and chromosome segregation. Nature *501*, 564–568.

Upadhya, P., Birkenmeier, E.H., Birkenmeier, C.S., and Barker, J.E. (2000). Mutations in a NIMA-related kinase gene, Nek1, cause pleiotropic effects including a progressive polycystic kidney disease in mice. Proc. Natl. Acad. Sci. USA *97*, 217–221.

Varmuza, S., Jurisicova, A., Okano, K., Hudson, J., Boekelheide, K., and Shipp, E.B. (1999). Spermiogenesis is impaired in mice bearing a targeted mutation in the protein phosphatase 1cgamma gene. Dev. Biol. *205*, 98–110.

Wiltshire, T., Park, C., Caldwell, K.A., and Handel, M.A. (1995). Induced premature G2/M-phase transition in pachytene spermatocytes includes events unique to meiosis. Dev. Biol. *169*, 557–567.

Yeo, A.J., Becherel, O.J., Luff, J.E., Graham, M.E., Richard, D., and Lavin, M.F. (2015). Senataxin controls meiotic silencing through ATR activation and chromatin remodeling. Cell Discov *1*, 15025.

Zhang, N., and Pati, D. (2012). Sororin is a master regulator of sister chromatid cohesion and separation. Cell Cycle *11*, 2073–2083.

Zhang, J., Hakansson, H., Kuroda, M., and Yuan, L. (2008). Wapl localization on the synaptonemal complex, a meiosis-specific proteinaceous structure that binds homologous chromosomes, in the female mouse. Reprod. Domest. Anim. *43*, 124–126.

Cell Reports, Volume *17*

Supplemental Information

Cohesin Removal along the Chromosome Arms during the First Meiotic Division Depends on a NEK1-PP1γ-WAPL Axis in the Mouse

Miguel A. Brieño-Enríquez, Stefannie L. Moak, Melissa Toledo, Joshua J. Filter, Stephen Gray, José L. Barbero, Paula E. Cohen, and J. Kim Holloway

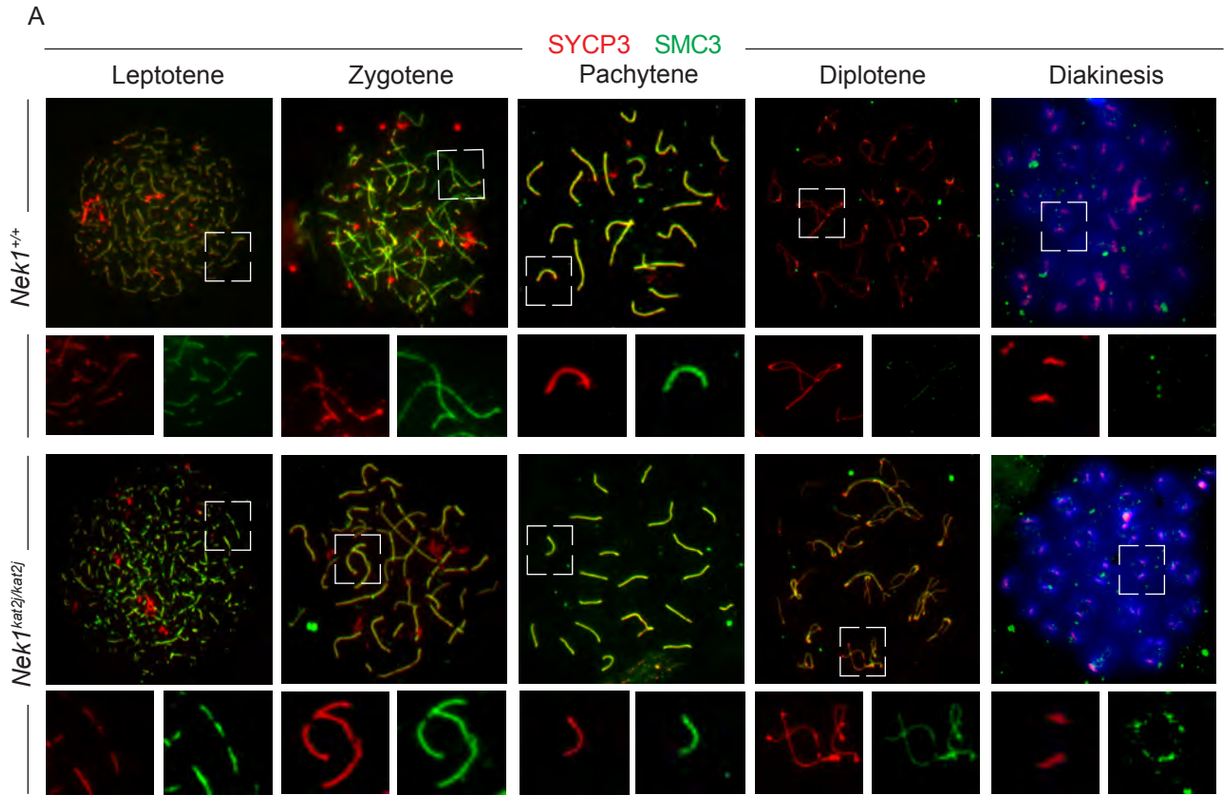

Figure S1. Related to figure 1- Loss of NEK1 induces retention of cohesin SMC3 during meiotic prophase I. A) IF against SMC3 (green) and SYCP3 (red) in Nek1$^{+/+}$ and Nek1$^{kat2j/kat2j}$ spermatocyte spreads. Loading of SMC3 onto chromosome cores in Nek1$^{+/+}$ starts at leptotene and is present until pachytene. At late pachytene and diplotene SMC3 is unload from chromosome cores. In Nek1$^{kat2j/kat2j}$ spermatocytes there is a retention of SMC3 that is observable at diplotene and continues to diakinesis.

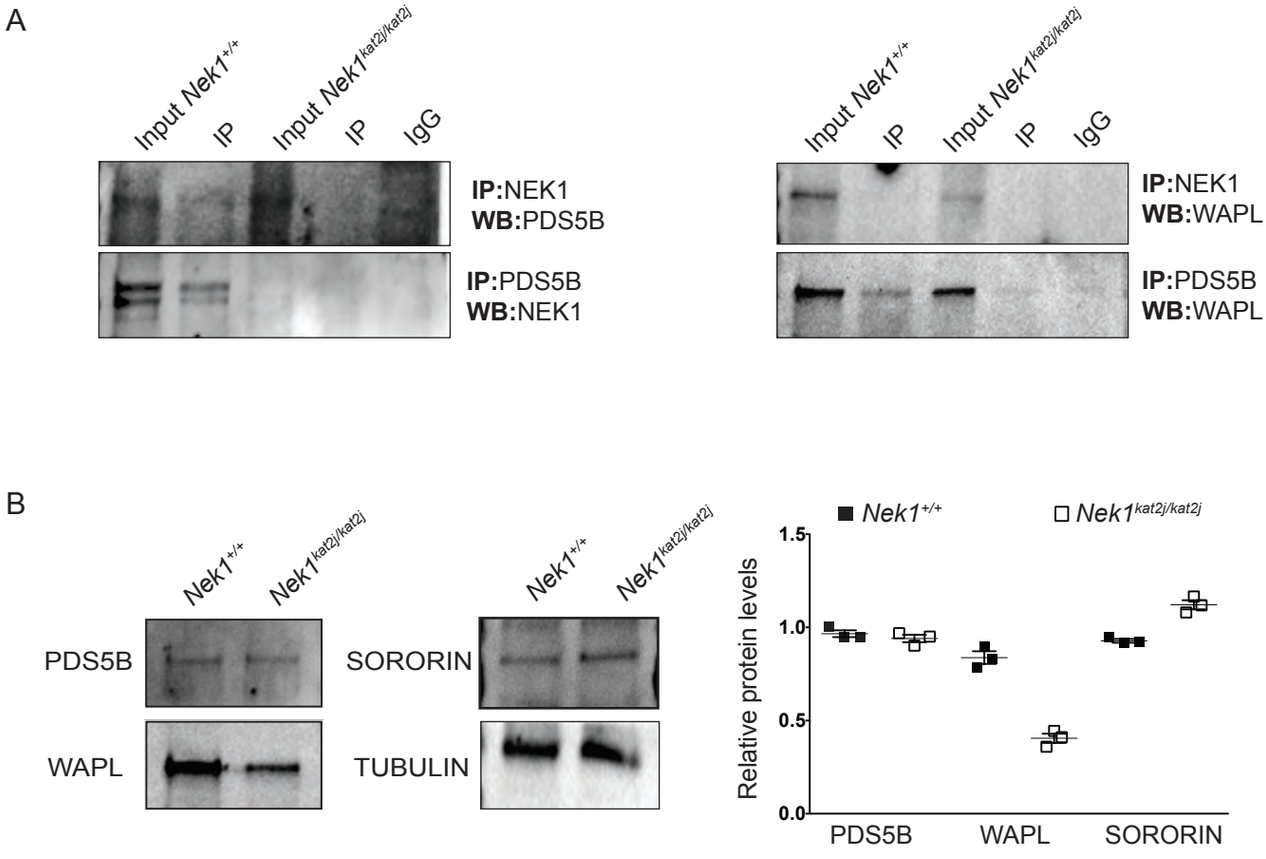

Figure S2. Related to Figure 2- Lack of NEK1 alters the prophase pathway proteins and their interactions in meiotic cells. A) Immunoprecipitation with NEK1 and PDS5B antibodies, followed by WB with antibodies against PDS5B, NEK1, or WAPL; B) Western blot against PDS5B, WAPL, Sororin, and Tubulin in protein extracts from isolated pachytene cells from Nek1$^{+/+}$ and Nek1$^{kat2j/kat2j}$ testes, with quantitation of protein levels relative to tubulin. Relative protein levels are given ± SD.

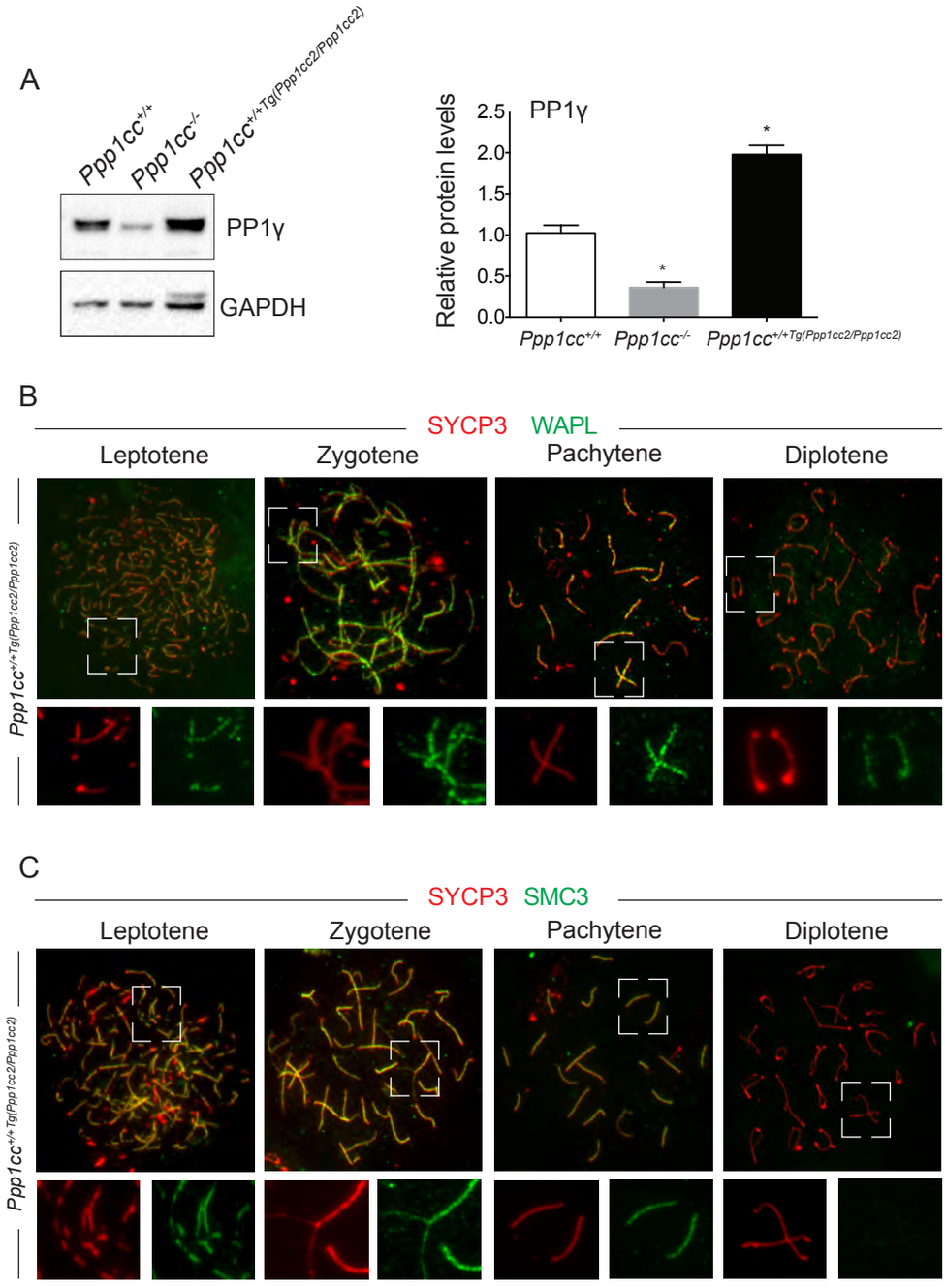

Figure S3. Related to Figure 3- Overexpression of PP1γ leads to retention of WAPL and premature release of SMC3 during meiotic prophase I. A) PP1γ protein levels in Ppp1cc$^{+/+}$, Ppp1cc$^{-/-}$ and Ppp1ccp$^{+/+Tg(Ppp1cc2/Ppp1cc2)}$ in whole testis lysate relative to GAPDH. Relative protein levels are given ± SD; B) IF against WAPL (green) and SYCP3 (red) in Ppp1ccp$^{+/+Tg(Ppp1cc2/Ppp1cc2)}$ spermatocyte spreads. Localization of WAPL along the different stages of meiotic prophase in PP1γ shows a retention of WALP during diplotene: C) IF against SMC3 (green) and SYCP3 (red) in Ppp1ccp$^{+/+Tg(Ppp1cc2/Ppp1cc2)}$ spermatocyte spreads. Overexpression of PP1γ induces a premature removal of SMC3 during pachytene-diplotene.

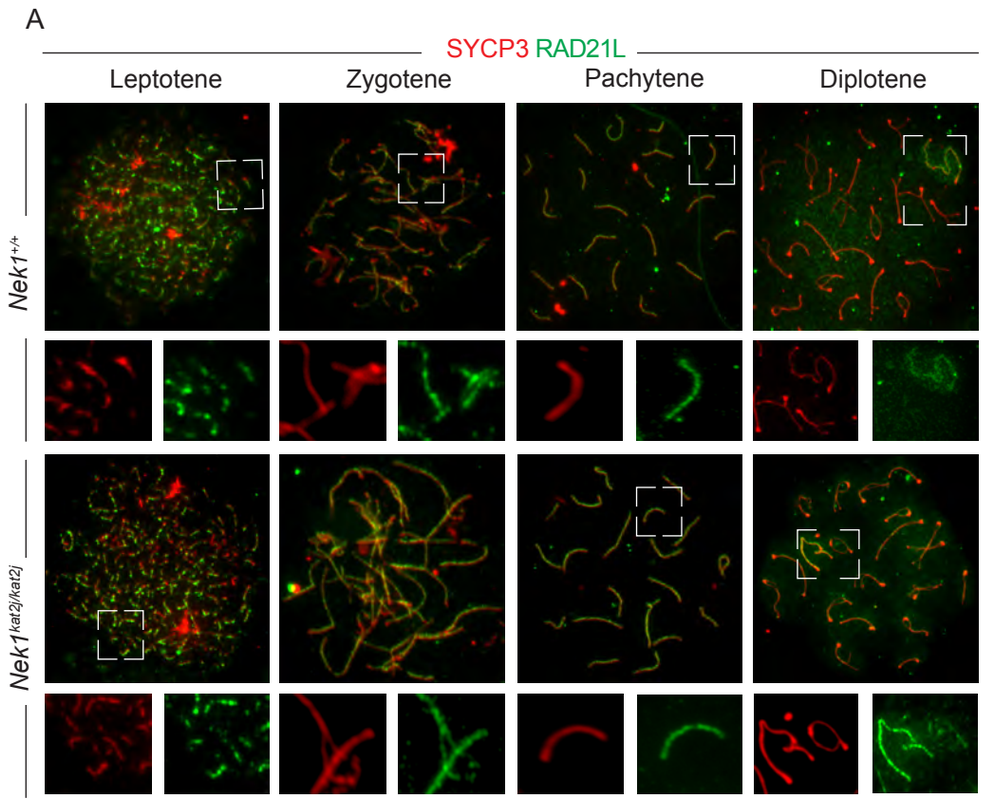

Figure S4. Related to Figure 1- Loss of NEK1 induces retention of RAD21L during diplotene of prophase I. A) IF against RAD21L (green) and SYCP3 (red) in Nek1$^{+/+}$ and Nek1$^{kat2j/kat2j}$ spermatocyte spreads. In Nek1$^{+/+}$ spermatocytes the loading of RAD21L onto chromosome cores from leptotene to pachytene. At late pachytene RAD21L is unload from chromosome cores except in the XY chromosomes. At diplotene Nek1$^{kat2j/kat2j}$ spermatocytes showed retention of RAD21L on XY chromosome cores as well as in autosome chromosome cores.

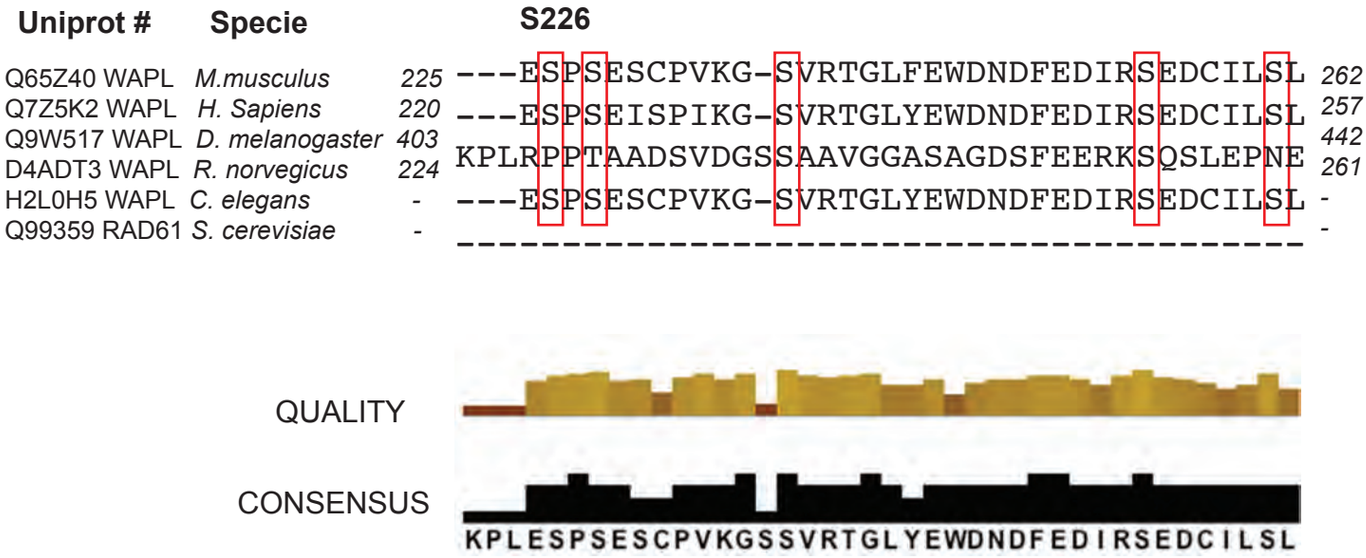

Figure S5. Analysis of protein sequence homology using CLUSTALOWS by Jalview 2.90b2. Alignment of WAPL (RAD61) sequences across organisms using Jalview. Sequences were obtained from Uniprot (http://www.uniprot.org/). Red squares indicate conserved serines in a serine-rich domain.

SUPPLEMENTAL TABLE LEGENDS

Supplemental Table 1. Related to Figure 1- Phosphoproteomics mass spectrophotometry data

Supplemental Table 2. Related to Figure 2- Immunoprecipitation with NEK1 antibody followed by mass spectrophotometry analysis

Supplemental Table 3. Related to Figure 2- Immunoprecipitation with WAPL antibody followed by mass spectrophotometry analysis